

Treating London-Dispersion Effects with the Latest Minnesota Density Functionals: Problems and Possible Solutions

Lars Goerigk*

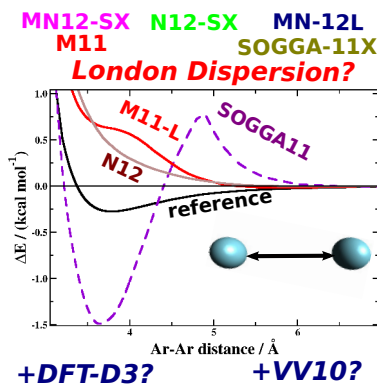
School of Chemistry, The University of Melbourne, Victoria 3010, Australia

E-mail: lars.goerigk@unimelb.edu.au

Abstract

It is shown that the latest Minnesota density functionals (SOGGA11, M11-L, N12, MN12-L, SOGGA11-X, M11, N12-SX, and MN12-SX) do not properly describe London-dispersion interactions. Grimme's DFT-D3 correction can solve this problem partially, however, double-counting of medium-range electron correlation can occur. For the related M06-L functional, the alternative VV10 van-der-Waals kernel is tested, but it experiences similar double-counting. Most functionals give unphysical dissociation curves for the argon dimer, an indication for method-inherent problems, and further investigation is recommended. These results are further evidence that the London-dispersion problem in density functional theory approximations is unlikely to be solved by mere empirical optimization of functional parameters, unless the functionals contain components that ensure the correct asymptotic long-range behavior. London dispersion is ubiquitous, which is why the reported findings are not only important for theoreticians, but also a reminder to the general chemist to carefully consider their choice of method before undertaking computational studies.

TOC Graphic



Keywords: density functional theory, Minnesota density functionals, London dispersion, noncovalent interactions, DFT-D3, DFT-NL, vdW-DFT

Herein, we investigate if the latest Minnesota-type¹⁻⁷ density-functional-theory approximations (DFTAs) can describe the ubiquitous London-dispersion⁸ phenomenon. It has been shown that these methods are a substantial improvement over their immensely popular predecessors, the M05 and M06 suites of functionals,⁹⁻¹¹ not only for general molecular chemistry, but also for solid-state physics.¹² Very promising are the new range-separated hybrids M11¹ and MN12-SX,² as well as their local counterparts M11-L³ and MN12-L.⁴ These functionals all include terms that depend on the kinetic-energy density. In addition, also related methods relying only on the density and its gradient have been developed: the global hybrid SOGGA11-X,⁵ the range-separated hybrid N12-SX,² and their local versions SOGGA11⁶ and N12.⁷

In the strictest sense, London dispersion refers to attractive electron correlation effects between noncovalently bound moieties whose electron clouds do not overlap. In this long-range regime, the interaction energy is governed by the famous R^{-6} tail, with R being the distance between the involved moieties.⁸ On the other hand, attractive medium-range effects around the van-der-Waals minimum are also sometimes labeled as "dispersion". In this regime, partial overlap of the individual electron clouds cannot be neglected. Herein, we consider both regimes and we use the terms medium- and long-range dispersion accordingly.

Like their predecessors, the latest Minnesota functionals are examples for attempts to incorporate medium-range dispersion through empirical fitting of a large number of functional parameters to a diverse set of benchmark data. This training set includes a subset of 31 noncovalent interaction energies (NCIEs) in which 7 systems are dominated by "weak interactions" and 5 more by " $\pi - \pi$ stacking". Based on an analysis of this subset, particularly the M11, MN12-SX, and MN12-L functionals were recommended as some of the best performing for NCIEs.¹² However, due to the small number of test cases, knowledge of their capability to describe London dispersion is limited. It was reported recently that the two M11-type DFTAs underbind the helium, argon, coronene and naphthalene dimers,^{13,14} and that M11 and N12 were unable to properly describe adsorption of aromatic systems on graphene.¹⁵

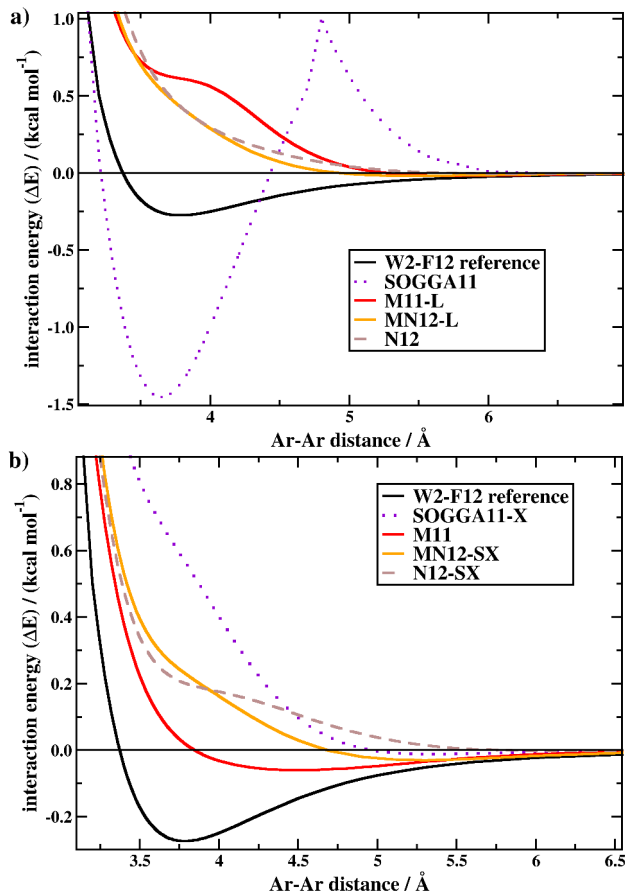


Figure 1: Dissociation curves of the argon dimer for local (a) and for hybrid Minnesota DFTAs (b) obtained with the AVQZ AO basis set and Gaussian’s ”superfine” quadrature grid. The reference curve was obtained at the nonrelativistic W2-F12 level of theory.

Given the tremendous success of their predecessors, it is expected that also the new Minnesota methods will soon be applied regularly by the broader research community. In light of this, a comprehensive analysis of all these methods for London-dispersion interactions is needed to complement our understanding of their applicability.

We begin our discussion with the dissociation curve of the argon dimer. Results for the investigated DFTAs with the large aug-cc-pVQZ¹⁶ (AVQZ) atomic-orbital (AO) quadruple- ζ basis set are compared with the accurate composite W2-F12¹⁷ level of theory (Figs. 1a and 1b). It turns out that almost all functionals are nonbinding. Only the MN12-L and N12 functionals show the smooth exponential decay expected for a conventional DFTA that is unable to describe medium- and long-range dispersion

(Fig. 1a). The curve for M11-L has an unphysical inflection point in the van-der-Waals region; something that has also been observed before.¹³ Herein, we report that also the SOGGA-11X, N12-SX and MN12-SX curves have inflection points, albeit with less pronounced changes in curvature (Fig. 1b). SOGGA11 shows a very unusual dissociation behavior: first, it overshoots the binding energy by more than a factor of 5 before it becomes strongly repulsive at around 5Å (Fig. 1a). M11 is the only functional that somewhat binds the dimer, however, the binding energy is underestimated by a factor of almost 5 and the optimal Ar-Ar distance is by 0.8 Å too long (Fig. 1b).

For previous Minnesota functionals, an unpredictable quadrature-grid dependence has been reported,^{18,19} something that has inspired the recent suggestion to impose grid sensitivity as a constraint in DFTA fitting procedures.²⁰ Initial attempts with Gaussian’s²¹ large ”ultrafine” (99,590) Lebedev quadrature grid produced wiggly dissociation curves for the argon dimer for nearly all methods (Fig. S1 in the Supporting Information, SI). Therefore, the results for Fig. 1 were obtained with Gaussian’s ”superfine” (150,974) Lebedev grid. Additional double-checks with the NWCHEM²² program and its largest quadrature grid confirmed the unusual form of the SOGGA11 curve, thus ruling out any grid dependencies as the culprit (Fig. S2). A more detailed analysis of the technicalities of grid dependencies should be reserved for a separate study.

To summarize, the initial results indicate that all investigated functionals have serious problems with the proper description of London-dispersion effects in the argon dimer. The unphysical results in the medium-range region are particularly worrisome, as the parameter fitting procedure was designed to mimic dispersion effects near van-der-Waals minima. In the remainder of this manuscript we will determine if this conclusion can be generalized.

The results for the argon dimer are surprising, as light rare-gas dimers were part of the initial parameter training set, and any problems with nonbinding behavior during the fitting process have not been reported.¹⁻⁷ Tab. 1 gives a likely explanation for this discrepancy by comparing the binding energies for the neon and argon dimers for

Table 1: Binding energies (kcal/mol) for the neon and argon dimers obtained with the MG3S and AVQZ AO basis sets. Reference values and geometries are taken from the RG6²³ benchmark set.

Functional	Ne ₂		Ar ₂	
	MG3S	AVQZ	MG3S	AVQZ
SOGGA11	1.44	-0.55	-1.50	-1.39
M11-L	0.18	0.49	0.25	0.62
MN12-L	0.01	0.18	0.18	0.45
N12	-0.08	0.10	0.44	0.45
SOGGA11-X	0.01	0.22	0.50	0.59
M11	-0.11	-0.08	-0.16	0.03
MN12-SX	-0.03	0.11	-0.03	0.24
N12-SX	-0.07	0.07	0.11	0.21
Ref.	-0.08		-0.28	

AVQZ with the smaller triple- ζ MG3S²⁴ basis set. MG3S was used in the functionals' parameter optimization without applying any corrections for basis-set superposition error (BSSE). In nearly all cases, MG3S induces an additional stabilization of 0.2 kcal/mol or more compared to AVQZ (Tab. 1). At the MG3S level, N12, M11, MN12-SX and N12-SX appear to be in excellent agreement with the reference value of -0.08 kcal/mol for the neon dimer. The likely explanation is that the BSSE is the source for this good result and that it does not stem from any functional-specific components. Remarkably, SOGGA11 shows the reverse behavior for the neon dimer; it is unbound for MG3S and too strongly bound for AVQZ. Note that unusually high BSSEs even for very large AO basis sets have been reported for the M06 and M11 suites of functionals and they were attributed to the magnitude of the inhomogeneity correction factors in the respective exchange parts.²⁵ The extent of BSSE for both dimers and basis sets is further analyzed in Tab. S3, and we can conclude that also the SOGGA11, N12 and MN12 classes of functionals suffer from BSSE even with the relatively large AVQZ AO basis set.

Next, we turn our attention to Hobza's S66x8 benchmark set,²⁷ which comprises 66 different noncovalently bound dimers at eight different intermolecular distances. These are defined by intermolecular distance multipliers (IDMs) relative to each dimer's

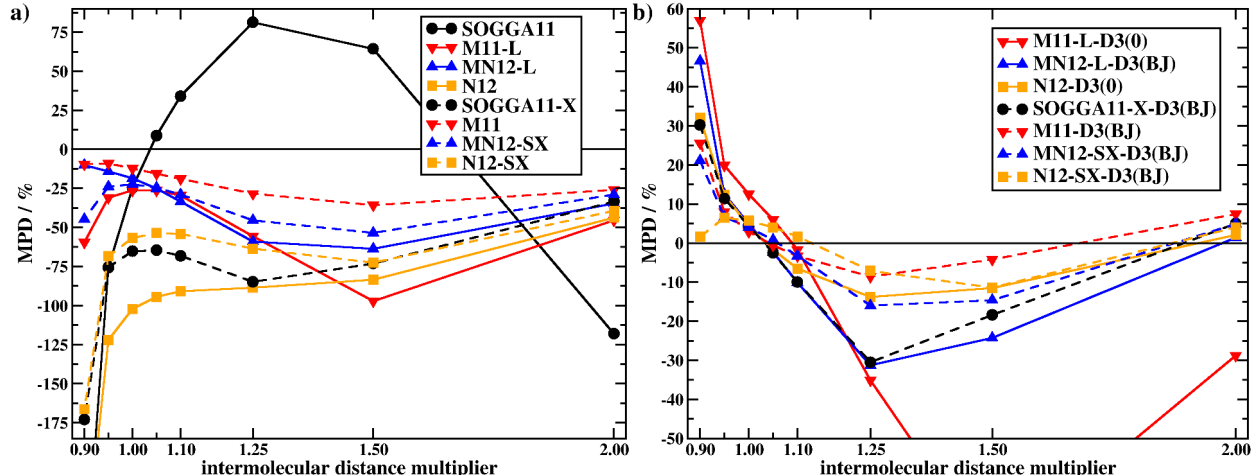


Figure 2: Mean percentage deviations (MPDs) for S66x8 (kcal/mol) for dispersion uncorrected (a) and corrected (b) Minnesota functionals. All results are based on calculations with the def2-QZVP²⁶ quadruple- ζ AO basis set. Negative MPDs indicate underbinding.

equilibrium distance ranging from IDM=0.9 to IDM=2.0. The particular value of S66x8 was shown in a study by Grimme and co-workers who demonstrated that the M05 and M06 suites of functionals were underbinding in the long-distance region.²⁸ Similarly to their study, we carry out the present analysis with the help of mean percentage deviations (MPDs) obtained separately for each IDM:²⁸

$$MPD = \frac{100}{n} \sum_n \frac{\Delta E_{functional} - \Delta E_{reference}}{\Delta E_{reference}}, \quad (1)$$

where the summation index n goes over all 66 systems. ΔE is the energy for the decomposition of a dimer into its monomers; hence, a negative MPD indicates an underbinding tendency.

Exactly such a tendency is observed for almost all of the investigated DFTAs (Fig. 2a). For most methods, the MPDs are closest to zero in the equilibrium-distance region. However, the best functional in this region still has an MPD of -12.2% for IDM=1.0 (M11), while MN12-L, MN12-SX and M11-L underbind the dimers by about 19 to 26%. This underbinding tendency increases for longer intermolecular distances, with values ranging from -36 to -97% (IDM=1.5) and from -26 to -46% (IDM=2.0). N12, N12-SX, and SOGGA11-X are highly repulsive at short distances with MPDs as

low as -267% (N12). SOGGA11 shows a peculiar trend with a strong underestimation at short and long distances (-281% and -118% , respectively), and with a large overestimation in between.

S66x8 can be separated into dimers that are predominantly bound by electrostatic interactions (hydrogen bonds), dispersion interactions or a mixture of both. The relevant MPDs listed in Tabs. S5-S7 show that most functionals underbind all three types of complexes. It is also possible to define mean absolute percentage deviations (MAPDs). For M11, these range between 11 and 52% (Fig. S4), while the other methods show significantly larger values of up to 282% (SOGGA11).

Grimme and co-workers combined the M05 and M06 classes with the DFT-D3 dispersion correction and they reported improvements, particularly in the long-range region.^{19,28} There are two forms of the DFT-D3 correction, the zero-damping variant DFT-D3(0)²³ and the Becke-Johnson-damping²⁹ variant DFT-D3(BJ)³⁰ (see SI). The M05 and M06 classes of functionals were almost all incompatible with DFT-D3(BJ) due to double-counting effects in the medium-range region, and it was recommended to use DFT-D3(0) instead.¹⁹ Herein, we attempted to fit both types of DFT-D3 to the eight recent Minnesota functionals. SOGGA11 is incompatible with either of the two versions, DFT-D3(0) works on average better with M11-L and N12, and DFT-D3(BJ) should be used for the remaining functionals (Tabs. S1 and S2).

The MPDs for S66x8 for DFT-D3-corrected functionals are shown in Fig. 2b. In most cases, absolute errors in the long-range region are reduced and for IDM=2.0 a slight overestimation of the binding energies by up to 10% is observed. Particularly the M11 and N12-SX functionals benefit from the dispersion correction, and the MPDs are usually within $\pm 10\%$ between IDM=0.95 and IDM=2.0. However, for most functionals an overestimation of up to 60% is observed for short distances, most likely due to double-counting effects. This is particularly the case for the dispersion-dominated and mixed complexes (Tabs. S6 and S7), while the dispersion correction improves the hydrogen-bonded complexes for all IDMs (Tab. S5). Overall, M11-L seems to benefit the least from the DFT-D3 correction (Fig. 2b).

Tab. 2 shows mean absolute deviations (MADs) over the whole set of the 528 interaction energies in S66x8. DFT-D3 improves the results for the Minnesota functionals significantly: the best two values are 0.26 kcal/mol and 0.36 kcal/mol for the dispersion-corrected hybrids M11-D3(BJ) and N12-SX-D3(BJ). Conceptually, these methods belong to the fourth rung of Perdew’s Jacob’s-Ladder scheme.³¹ Interestingly, previous studies of the new Minnesota methods have always excluded the fifth-rung class of double-hybrid DFTAs,^{32,33} even though it has been established that dispersion-corrected double hybrids belong to the most accurate DFTAs for NCIEs.^{19,33} Herein, we report the first direct comparison between the new Minnesota functionals and the dispersion-corrected B2-PLYP-D3(BJ)³² double-hybrid (Tab. 2); its MAD is with 0.16 kcal/mol lower than for the best dispersion-corrected Minnesota functionals. In fact, this value is the lowest-reported value for S66x8 in the literature.²⁸

Tab. 2 also lists MADs for various benchmark sets that were part of the DFT-D3 fitting procedure. These cover NCIEs of dimers in their equilibrium geometries and relative energies of conformers of organic- and biochemical interest. Besides the separate MADs for each test set, the table also shows weighted MADs (WMADs) averaged over the three dimer test sets RG6, S22B and ADIM6, as well as WMADs averaged over the four conformer sets (see SI for details). From the MADs and WMADs it can be seen that in some cases, particularly for the conformers, the values increase for the dispersion-corrected methods, indicating double-counting in the medium-range region. SOGGA11-X-D3(BJ) is the only functional showing consistent improvement both for the dimers and the conformers. However, none of the functionals surpass B2PLYP-D3(BJ), which yields the lowest values in the table. Finally note that DFT-D3 cannot fix any functional-inherent errors that may contribute to the unusual shapes of the argon-dimer dissociation curves (Fig. S3).

Thus, also the latest Minnesota DFTAs can be improved with the DFT-D3 correction, with the drawback of possible medium-range double-counting. It is interesting to determine if this problem also occurs for a different form of dispersion correction. In 2010, Van Voorhis and Vydrov developed the VV10 van-der-Waals DFTA that com-

Table 2: Mean absolute deviations (MADs) and weighted MADs (WMADs) in kcal/mol for different DFTAs and various benchmark sets obtained with the def2-QZVP quadruple- ζ AO basis set.

Functional	S66x8	RG6 ^a	S22B ^b	ADIM6 ^c	ACONF ^d	SCONF ^e	CYCONF ^f	PCONF ^g	WMAD ^h _{dim}	WMAD ⁱ _{conf}
SOGGA11	1.92	0.53	3.27	1.28	1.71	4.07	0.68	4.92	2.44	2.90
M11-L	1.11	0.70	1.37	0.72	0.21	0.96	0.43	0.59	1.14	0.57
M11-L-D3(0)	0.68	0.35	0.72	1.47	0.17	0.52	0.52	2.15	0.79	0.73
MN12-L	0.90	0.68	1.08	0.52	0.65	0.56	0.44	3.11	0.91	1.05
MN12-L-D3(BJ)	0.66	0.32	1.00	1.10	0.78	0.58	0.49	3.83	0.90	1.25
N12	2.69	1.13	3.96	6.38	0.90	0.38	0.79	4.75	3.89	1.45
N12-D3(0)	0.54	0.12	0.86	0.24	0.10	1.05	0.73	0.91	0.62	0.69
SOGGA11-X	1.90	0.90	2.58	4.13	0.44	0.62	0.29	1.76	2.56	0.72
SOGGA11-X-D3(BJ)	0.40	0.27	0.62	0.32	0.30	0.31	0.14	0.94	0.51	0.40
M11	0.44	0.43	0.65	0.29	0.67	0.55	0.33	0.86	0.55	0.60
M11-D3(BJ)	0.26	0.15	0.41	0.79	0.73	0.57	0.35	1.23	0.43	0.70
MN12-SX	0.87	0.48	1.16	1.20	0.06	0.87	0.23	1.06	1.05	0.55
MN12-SX-D3(BJ)	0.37	0.20	0.66	0.42	0.23	0.79	0.21	1.92	0.54	0.73
N12-SX	1.60	0.71	2.36	3.55	0.53	0.52	0.49	2.79	2.28	0.95
N12-SX-D3(BJ)	0.36	0.09	0.58	0.14	0.04	0.34	0.56	0.71	0.42	0.37
M06-L	0.49	0.44	0.81	0.24	0.47	0.39	0.38	0.98	0.64	0.52
M06-L-D3(0)	0.30	0.44	0.44	0.91	0.51	0.41	0.36	1.18	0.52	0.58
M06-L-NL	0.26	0.33	0.39	1.01	0.58	0.43	0.43	1.49	0.49	0.68
B2-PLYP-D3(BJ) ^j	0.16	0.06	0.26	0.22	0.02	0.25	0.11	0.28	0.22	0.16

^a6 rare-gas dimers. ²³ ^b22 noncovalently bound dimers. ^{34,35} ^c6 alkane dimers. ²³ ^d18 alkane conformers. ³⁶ ^e19 sugar conformers. ³⁷ ^f11 cysteine conformers. ³⁸ ^g11 tripeptide conformers. ³⁹ ^hWeighted MAD averaged over the three test sets with dimers in equilibrium geometries (RG6, S22B, ADIM6; see SI). ⁱWeighted MAD averaged over four conformer test sets (see SI). ^jTaken from Refs. 28 and 30; note that the results for S22 are based on slightly different reference values.

combines a conventional semi-local exchange-correlation functional with a nonlocal (NL), electron-density-dependent correlation kernel that ensures the asymptotically correct description of London dispersion.⁴⁰ Later, Hujo and Grimme showed that this kernel can be successfully used with a variety of different semi-local DFTAs and they dubbed this approach DFT-NL.⁴¹ Although these studies fitted the VV10 kernel to the NCIEs of the S22 set only, it was shown that this choice of training procedure did not have any negative impact on the DFTAs’ results for thermochemistry (TC).^{41,42} Mardirossian and Head-Gordon recently demonstrated the full potential of the VV10-kernel by including it during the fitting procedures of their range-separated hybrid ω B97X-V¹³ and their meta-GGA functional B97M-V.²⁰ These DFTAs showed highly promising performance for NCIEs and TC, e.g. the MADs for S22 and S66x8 were 0.23 and 0.22 kcal/mol for ω B97X-V/aug-cc-pVTZ, while B97M-V/aug-cc-pVTZ yielded values of 0.23 and 0.17 kcal/mol, respectively.²⁰

At this stage, the new Minnesota functionals and the VV10 kernel are parts of separate programs, which is why we herein only conduct a preliminary study on the related M06-L¹⁰ combined with the VV10 kernel (M06-L-NL). Nevertheless, the results

for M06-L-NL give us a reliable first insight into the potential of using this correction for the newer functionals, given that they seem to suffer from similar problems as their predecessors. The MADs for the various benchmark sets in Tab. 2 indicate that M06-L-NL behaves similarly to M06-L-D3(0): while the values for S66x8 and S22B are significantly lower than for M06-L, the limited improvement and the sometimes increased MADs for the other benchmark sets are an indication that the DFT-NL correction also induces double-counting with Minnesota-type functionals. The MPDs and MAPDs of M06-L-NL for S66x8 are shown in the SI (Fig. S5) and they are better than DFT-D3(0) for IDM=1.0, but worse for larger IDMs. We also report that combining DFT-NL with the M06-2X¹¹ hybrid was unsuccessful. Based on these preliminary results it is questionable whether combining the newer Minnesota functionals with the VV10 kernel could improve any of their underlying problems without a complete refit of their functional-inherent parameters.

In summary, we have demonstrated that the latest Minnesota-type DFTAs do not properly describe medium- and long-range London-dispersion interactions. We recommend that this fact be taken into account by the general chemist that may consider applying these methods in their research. For theoretically oriented chemists, these findings are further evidence that the common strategy of fitting functional parameters to NCIEs is unlikely to succeed, unless the DFTA contains specific components that provide a physically correct description of dispersion (see Refs. 13 and 20 for promising examples). Also, using larger basis sets in the parameter-fitting procedure is recommended to prevent BSSE-related artifacts. The peculiar dissociation behavior of the argon dimer for most of the tested methods justifies closer investigation of their underlying components, an undertaking that in the long term may improve our understanding of Minnesota-type DFTAs and help in the development of new methods. In initial studies, the latest Minnesota functionals have shown good performance for other chemical properties.¹² The next logical step is to analyze to what extent these other properties are influenced by the herein reported findings. These investigations are currently underway.

General Information. Gaussian09 Rev D.01²¹ with the large "ultrafine" quadrature grid was used in most cases, except for the rare-gas dimers, for which the larger "superfine" grid was applied. M06-L and DFT-NL calculations, in the post-self-consistent-field version,⁴⁰ were carried out with ORCA.3.0.2⁴³ with its options "grid7" and "vdw-grid4", and with the resolution-of-the-identity approximation for the Coulomb term.⁴⁴ DFT-D3^{23,30} corrections were obtained with Grimme's standalone code.⁴⁵ MOLPRO 2012.1⁴⁶ was used for nonrelativistic, zero-point-exclusive W2-F12¹⁷ calculations.

Acknowledgement

This work was funded by the Australian Research Council with a Discovery Early Career Researcher Award to L. G. (project number DE140100550). L. G. also acknowledges generous allocation of computing time from the National Computational Infrastructure (NCI) National Facility within the National Computational Merit Allocation Scheme (project fk5).

Supporting Information Available

Details on the DFT-D3 and DFT-NL methods; additional details on the argon-dimer dissociation curves; details on BSSE in Ne₂ and Ar₂; all statistical values for the various benchmark sets. This material is available free of charge via the Internet at <http://pubs.acs.org/>.

References

- (1) Peverati, R.; Truhlar, D. G. Improving the Accuracy of Hybrid Meta-GGA Density Functionals by Range Separation. *J. Phys. Chem. Lett.* **2011**, *2*, 2810–2817.
- (2) Peverati, R.; Truhlar, D. G. Screened-Exchange Density Functionals with Broad

- Accuracy for Chemistry and Solid-State Physics. *Phys. Chem. Chem. Phys.* **2012**, *14*, 16187–16191.
- (3) Peverati, R.; Truhlar, D. G. M11-L: A Local Density Functional That Provides Improved Accuracy for Electronic Structure Calculations in Chemistry and Physics. *J. Phys. Chem. Lett.* **2012**, *3*, 117–124.
- (4) Peverati, R.; Truhlar, D. G. An Improved and Broadly Accurate Local Approximation to the Exchange-Correlation Density Functional: The MN12-L Functional for Electronic Structure Calculations in Chemistry and Physics. *Phys. Chem. Chem. Phys.* **2012**, *14*, 13171–13174.
- (5) Peverati, R.; Truhlar, D. G. A Global Hybrid Generalized Gradient Approximation to the Exchange-Correlation Functional that Satisfies the Second-Order Density-Gradient Constraint and Has Broad Applicability in Chemistry. *J. Chem. Phys.* **2011**, *135*, 191102.
- (6) Peverati, R.; Zhao, Y.; Truhlar, D. G. Generalized Gradient Approximation That Recovers the Second-Order Density-Gradient Expansion with Optimized Across-The-Board Performance. *J. Phys. Chem. Lett.* **2011**, *2*, 1991–1997.
- (7) Peverati, R.; Truhlar, D. G. Exchange-Correlation Functional with Good Accuracy for Both Structural and Energetic Properties While Depending Only on the Density and Its Gradient. *J. Chem. Theory Comput.* **2012**, *8*, 2310–2319.
- (8) London, F. Zur Theorie und Systematik der Molekularkräfte. *Z. Phys.* **1930**, *63*, 245–279.
- (9) Zhao, Y.; Schultz, N. E.; Truhlar, D. G. Design of Density Functionals by Combining the Method of Constraint Satisfaction with Parametrization for Thermochemistry, Thermochemical Kinetics, and Noncovalent Interactions. *J. Chem. Theory Comput.* **2006**, *2*, 364–382.

- (10) Zhao, Y.; Truhlar, D. G. A New Local Density Functional for Main-Group Thermochemistry, Transition Metal Bonding, Thermochemical Kinetics, and Noncovalent Interactions. *J. Chem. Phys.* **2006**, *125*, 194101.
- (11) Zhao, Y.; Truhlar, D. G. The M06 Suite of Density Functionals for Main Group Thermochemistry, Thermochemical Kinetics, Noncovalent Interactions, Excited States, and Transition Elements: Two New Functionals and Systematic Testing of Four M06-Class Functionals and 12 Other Functionals. *Theor. Chem. Acc.* **2008**, *120*, 215–241.
- (12) Peverati, R.; Truhlar, D. G. Quest for a Universal Density Functional: The Accuracy of Density Functionals Across a Broad Spectrum of Databases in Chemistry and Physics. *Philos. Trans. R. Soc., A* **2014**, *372*, 20120476.
- (13) Mardirossian, N.; Head-Gordon, M. ω B97X-V: A 10-Parameter, Range-Separated Hybrid, Generalized Gradient Approximation Density Functional with Nonlocal Correlation, Designed by a Survival-Of-The-Fittest Strategy. *Phys. Chem. Chem. Phys.* **2014**, *16*, 9904–9924.
- (14) DiLabio, G. A.; Otero-de-la-Roza, A. Noncovalent Interactions in Density-Functional Theory. *ArXiv E-Prints* **2014**, arXiv:1405.1771 (accessed on 14 July 2015).
- (15) Wang, W.; Sun, T.; Zhang, Y.; Wang, Y.-B. Benchmark Calculations of the Adsorption of Aromatic Molecules on Graphene. *J. Comput. Chem.* **2015**, *36*, 1763–1771.
- (16) Woon, D. E.; Dunning, T. H. Gaussian Basis Sets for Use in Correlated Molecular Calculations. III. The Atoms Aluminum Through Argon. *J. Chem. Phys.* **1993**, *98*, 1358–1371.
- (17) Karton, A.; Martin, J. M. L. Explicitly Correlated Wn Theory: W1-F12 and W2-F12. *J. Chem. Phys.* **2012**, *136*, 124114.

- (18) Johnson, E. R.; Becke, A. D.; Sherrill, C. D.; DiLabio, G. A. Oscillations in Meta-Generalized-Gradient Approximation Potential Energy Surfaces for Dispersion-Bound Complexes. *J. Chem. Phys.* **2009**, *131*, 034111.
- (19) Goerigk, L.; Grimme, S. A Thorough Benchmark of Density Functional Methods for General Main Group Thermochemistry, Kinetics, and Noncovalent Interactions. *Phys. Chem. Chem. Phys.* **2011**, *13*, 6670–6688.
- (20) Mardirossian, N.; Head-Gordon, M. Mapping the Genome of Meta-Generalized Gradient Approximation Density Functionals: The Search for B97M-V. *J. Chem. Phys.* **2015**, *142*, 074111.
- (21) Gaussian 09 Revision D.01. Frisch, M. J.; Trucks, G. W.; Schlegel, H. B.; Scuseria, G. E.; Robb, M. A.; Cheeseman, J. R.; Scalmani, G.; Barone, V.; Mennucci, B.; Petersson, G. A.; et al. Gaussian, Inc., Wallingford CT, 2009.
- (22) Valiev, M.; Bylaska, E. J.; Govind, N.; Kowalski, K.; Straatsma, T. P.; Van Dam, H. J. J.; Wang, D.; Nieplocha, J.; Apra, E.; Windus, T. L. et al. NWChem: A Comprehensive and Scalable Open-Source Solution for Large Scale Molecular Simulations. *Comput. Phys. Commun.* **2010**, *181*, 1477 – 1489.
- (23) Grimme, S.; Antony, J.; Ehrlich, S.; Krieg, H. A Consistent and Accurate Ab Initio Parametrization of Density Functional Dispersion Correction (DFT-D) for the 94 Elements H-Pu. *J. Chem. Phys.* **2010**, *132*, 154104.
- (24) Lynch, B. J.; Zhao, Y.; Truhlar, D. G. Effectiveness of Diffuse Basis Functions for Calculating Relative Energies by Density Functional Theory. *J. Phys. Chem. A* **2003**, *107*, 1384–1388.
- (25) Mardirossian, N.; Head-Gordon, M. Characterizing and Understanding the Remarkably Slow Basis Set Convergence of Several Minnesota Density Functionals for Intermolecular Interaction Energies. *J. Chem. Theory Comput.* **2013**, *9*, 4453–4461.

- (26) Weigend, F.; Ahlrichs, R. Balanced Basis Sets of Split Valence, Triple Zeta Valence and Quadruple Zeta Valence Quality for H to Rn: Design and Assessment of Accuracy. *Phys. Chem. Chem. Phys.* **2005**, *7*, 3297–3305.
- (27) Řezáč, J.; Riley, K. E.; Hobza, P. S66: A Well-balanced Database of Benchmark Interaction Energies Relevant to Biomolecular Structures. *J. Chem. Theory Comput.* **2011**, *7*, 2427–2438.
- (28) Goerigk, L.; Kruse, H.; Grimme, S. Benchmarking Density Functional Methods against the S66 and S66x8 Datasets for Non-Covalent Interactions. *ChemPhysChem* **2011**, *12*, 3421–3433.
- (29) Becke, A. D.; Johnson, E. R. A Density-Functional Model of the Dispersion Interaction. *J. Chem. Phys.* **2005**, *123*, 154101.
- (30) Grimme, S.; Ehrlich, S.; Goerigk, L. Effect of the Damping Function in Dispersion Corrected Density Functional Theory. *J. Comput. Chem.* **2011**, *32*, 1456–1465.
- (31) Perdew, J. P.; Schmidt, K. In *Density Functional Theory and Its Applications to Materials*; Doren, V. E. V., Alsenoy, C. V., Geerlings, P., Eds.; AIP Conference Proceedings; American Institute of Physics, 2001; Vol. 577; pp 1–20.
- (32) Grimme, S. Semiempirical Hybrid Density Functional with Perturbative Second-Order Correlation. *J. Chem. Phys.* **2006**, *124*, 034108.
- (33) Goerigk, L.; Grimme, S. Double-Hybrid Density Functionals. *Wiley Interdiscip. Rev.: Comput. Mol. Sci.* **2014**, *4*, 576–600.
- (34) Jurečka, P.; Šponer, J.; Černý, J.; Hobza, P. Benchmark Database of Accurate (MP2 and CCSD(T) Complete Basis Set Limit) Interaction Energies of Small Model Complexes, DNA Base Pairs, and Amino Acid Pairs. *Phys. Chem. Chem. Phys.* **2006**, *8*, 1985–1993.
- (35) Marshall, M. S.; Burns, L. A.; Sherrill, C. D. Basis Set Convergence of the Coupled-Cluster Correction, δ MP2CCSD(T): Best Practices for Benchmarking

- Non-Covalent Interactions and the Attendant Revision of the S22, NBC10, HBC6, and HSG Databases. *J. Chem. Phys.* **2011**, *135*, 194102.
- (36) Gruzman, D.; Karton, A.; Martin, J. M. L. Performance of Ab Initio and Density Functional Methods for Conformational Equilibria of C_nH_{2n+2} Alkane Isomers ($n = 4-8$). *J. Phys. Chem. A* **2009**, *113*, 11974–11983.
- (37) Goerigk, L.; Grimme, S. A General Database for Main Group Thermochemistry, Kinetics, and Noncovalent Interactions - Assessment of Common and Reparameterized (Meta-)GGA Density Functionals. *J. Chem. Theory Comput.* **2010**, *6*, 107–126.
- (38) Wilke, J. J.; Lind, M. C.; Schaefer III, H. F.; Császár, A. G.; Allen, W. D. Conformers of Gaseous Cysteine. *J. Chem. Theory Comput.* **2009**, *5*, 1511–1523.
- (39) Řeha, D.; Valdes, H.; Vondrášek,; Hobza, P.; Abu-Riziq, A.; Crews, B.; de Vries, M. S. Structure and IR Spectrum of Phenylalanyl-Glycyl-Glycine Tripeptide in the Gas-Phase: IR/UV Experiments, Ab Initio Quantum Chemical Calculations, and Molecular Dynamic Simulations. *Chem. Eur. J.* **2005**, *11*, 6803–6817.
- (40) Vydrov, O. A.; Van Voorhis, T. Nonlocal Van Der Waals Density Functional: The Simpler the Better. *J. Chem. Phys.* **2010**, *133*, 244103.
- (41) Hujo, W.; Grimme, S. Performance of the Van Der Waals Density Functional VV10 and (Hybrid)GGA Variants for Thermochemistry and Noncovalent Interactions. *J. Chem. Theory Comput.* **2011**, *7*, 3866–3871.
- (42) Goerigk, L. How do DFT-DCP, DFT-NL, and DFT-D3 Compare for the Description of London-Dispersion Effects in Conformers and General Thermochemistry? *J. Chem. Theory Comput.* **2014**, *10*, 968–980.
- (43) Neese, F. The ORCA Program System. *Wiley Interdiscip. Rev.: Comput. Mol. Sci.* **2012**, *2*, 73–78.

- (44) Eichkorn, K.; Treutler, O.; Öhm, H.; Häser, M.; Ahlrichs, R. Auxiliary Basis Sets to Approximate Coulomb Potentials. *Chem. Phys. Lett.* **1995**, *240*, 283 – 290.
- (45) DFT-D3 Web Site by the group of Prof. Stefan Grimme: <http://www.thch.uni-bonn.de/tc/index.php?section=downloadsubsection=DFT-D3&lang=english> (accessed on 24 July 2015).
- (46) Werner, H.-J.; Knowles, P. J.; Knizia, G.; Manby, F. R.; Schütz, M. Molpro: A General-Purpose Quantum Chemistry Program Package. *Wiley Interdiscip. Rev.: Comput. Mol. Sci.* **2012**, *2*, 242–253.